EuPA Open Proteomics 9 (2015) 43–53

Contents lists available at ScienceDirect

EuPA Open Proteomics

journal homepage: www.elsevier.com/locate/euprot

Enhancing cognate target elution efficiency in gel-free chemical proteomics

Branka Radic-Sarikas[a,3], Uwe Rix[a,b,3], Alexey Stukalov[a,1], Manuela Gridling[a], André C. Müller[a], Jacques Colinge[a,2], Giulio Superti-Furga[a,c], Keiryn L. Bennett[a,*]

[a] CeMM Research Center for Molecular Medicine of the Austrian Academy of Sciences, Vienna, Austria
[b] Department of Drug Discovery, H. Lee Moffitt Cancer Center & Research Institute, Tampa, FL, USA
[c] Center for Physiology and Pharmacology, Medical University of Vienna, Vienna, Austria

ARTICLE INFO

Article history:
Received 1 June 2015
Received in revised form 2 August 2015
Accepted 25 September 2015
Available online 30 September 2015

Keywords:
Chemical proteomics
Mass spectrometry gel-free
Double elution
Dasatinib
Sunitinib

ABSTRACT

Gel-free liquid chromatography mass spectrometry coupled to chemical proteomics is a powerful approach for characterizing cellular target profiles of small molecules. We have previously described a fast and efficient elution protocol; however, altered target profiles were observed. We hypothesised that elution conditions critically impact the effectiveness of disrupting drug-protein interactions. Thus, a number of elution conditions were systematically assessed with the aim of improving the recovery of all classes of proteins whilst maintaining compatibility with immunoblotting procedures. A double elution with formic acid combined with urea emerged as the most efficient and generically applicable elution method for chemical proteomics

1. Significance

The majority of drugs are surprisingly promiscuous, thus a powerful approach to characterize the cellular target profiles of small molecules is imperative. An acid-based chemical proteomic elution protocol compatible with gel-free liquid chromatography mass spectrometry (LCMS) is effective; however, altered target profiles were observed. We have optimised and implemented a new strategy that decidedly enhanced cognate target elution efficiency. This was evident for both chemical immobilization of compounds on an inert matrix and also for biotinylated compounds on avidin-functionalized resins.

2. Introduction

Understanding the molecular mechanisms of drugs is of utmost importance as this knowledge may guide target-based improvement of lead compounds; whilst revealing off-target effects that lead to toxicity [1–3]. If chemical entities could be matched to biological processes at the molecular level throughout the drug discovery and development process, the attrition rates for tool compounds and drugs could potentially decrease. Concomitantly, therapeutic efficacy should also improve. Thus, deciphering the target spectra of bioactive compounds can lead to exploitation of the full potential of drug candidates. Some examples where this is applicable are in aiding the identification of novel therapeutic applications or elucidating side effects [4–7]; and/or pharmacological tool compounds that are used to dissect complex biological processes [8]. There is a growing body of data that supports the notion that the majority of drugs are promiscuous and that the 'one drug, one target' paradigm seldom applies [9]. The more we understand drug properties, the more we realize that it is not so much the question of if a compound has off-targets, but how many there are and how these contribute to the biological effects. Several methods have been employed in the identification of small molecule-protein interactions, such as chemical proteomics or gene expression-based methods [3,5,10,11].

Abbreviations: MS, mass spectrometry; LC, liquid chromatography; LCMS, liquid chromatography mass spectrometry; iTRAQ, isobaric tags for relative and absolute quantitation; SDS, sodium dodecyl sulphate; CML, chronic myeloid leukemia; TEA, triethylamine; HPLC-MS, high-performance liquid chromatography mass spectrometry; TEAB, triethylammonium bicarbonate; FA, formic acid; ACN, acetonitrile; XX-NHS, biotin-biotinamidohexanoyl-6-aminohexanoic acid *N*-hydroxysuccinimide ester; DTT, dithiothreitol; TLCK, *N*-alpha-tosyl-L-lysinyl-chloromethylketone; U/FA, 3 M urea and 50 mM FA; B, boiling; dNSAF, distributed normalized spectral abundance factor; dSAF, spectral abundance factor; uSpC, unique spectral count.

* Corresponding author. CeMM Research Center for Molecular Medicine of the Austrian Academy of Sciences, Lazarettgasse 14, AKH BT25.3, Vienna, 1090 Austria.
E-mail address: kbennett@cemm.oeaw.ac.at (K.L. Bennett).
[1] Present address: Max-Planck Institute of Biochemistry, Am Klopferspitz 18, D-82152 Martinsried/Munich, Germany.
[2] Present address: Institut de Recherche en.Cancérologie de Montpellier, Campus Val d'Aurelle 34298 Montpellier, France.
[3] These authors equally contributed to this work.

http://dx.doi.org/10.1016/j.euprot.2015.09.002

Chemical proteomics is a post-genomic affinity chromatography-based approach that is enabled by modern mass spectrometry (MS) and bioinformatic capabilities [3,12–17]. There are various protocols in use, but the most widely-accepted procedure entails the elution of interacting proteins from a drug-affinity matrix with sodium dodecyl sulphate (SDS) followed by analysis of the eluate by one- or two-dimensional SDS-PAGE and *in situ* tryptic digestion of the proteins. In most cases, the resultant peptide mixture is analyzed by nano-liquid chromatography (LC) coupled to nano-electrospray (ESI) tandem MS[18]. Whereas this gel-based proteomic workflow (often referred to as GeLCMS) has been highly successful and has led to a number of landmark publications that describe several important novel drug-protein interactions [8,19–21], there are also a number of important limitations. These include high labor demand, high cost, and an increased risk of keratin contamination as a consequence of multiple sample handling steps. GeLCMS is also not directly compatible with quantitative proteomic approaches that utilize post-digestion chemical labeling with isobaric tags (*e.g.*, iTRAQ, TMT) [22]. Therefore, gel-free proteomic methods are receiving more widespread interest.

We have recently shown that adaptation of a gel-free approach resulted in a significant reduction in sample preparation and MS instrument time, and ultimately led to an increase in absolute numbers of identified proteins [23]. Target recovery was also improved such that a 5-fold decrease in the protein input was enabled without loss of data quality [23]. Furthermore, we have demonstrated the compatibility of our approach with subsequent relative quantitative proteomics using iTRAQ labeling [24,25]. Despite these advancements, the method has only been used in a few studies from our groups [26–30], as there were some questions raised concerning cognate target recovery (especially for receptor tyrosine kinases, RTKs) and decreased immunoblot efficiency. For example, the detection of the BCR-ABL fusion oncoprotein, which is the biochemical hallmark of chronic myeloid leukemia (CML) and a major drug target of several kinase inhibitors (*e.g.*, imatinib and dasatinib), was compromised. This observation was apparent with dot blots and western gel-based immunoblot assays. Therefore, we hypothesised that elution conditions critically impact the effectiveness of disrupting drug-protein interactions. Subsequently, the final drug-protein profile can be altered. Surprisingly, this aspect is rarely addressed and often overlooked in biochemical approaches linked to mass spectrometry-based proteomics. Thus, the ultimate aim of this current study was to systematically and thoroughly assess a number of different elution conditions to determine the best, yet generic, protocol that efficiently eluted a broad range of cognate targets encompassing several protein classes. Dasatinib was initially selected as the test compound. This drug is a multi-kinase inhibitor approved for the treatment of patients with imatinib-resistant CML and BCR-ABL-positive acute lymphoblastic leukemia (ALL). Dasatinib is not only a potent inhibitor of the large 210 kDa fusion protein BCR-ABL [31], but also of the cytosolic TEC family kinase BTK [6] and the membrane-bound receptor tyrosine kinase DDR1 [21]. In addition, we have previously generated a dasatinib analog suitable for chemical proteomics that we have validated and successfully employed in different studies [21,32,33].

A number of elution conditions were assessed with the objective to improve: (i) compatibility with immunoblot analysis, which is an important quality control; and (ii) the overall recovery of *bona fide* targets. The protocol optimised on the coupleable analog of dasatinib was further extended to a biotinylated derivative of the drug; and also to a second compound with a different target profile. Compared to dasatinib, sunitinib [34] inhibits a complementary fraction of kinases [28]. The drug is an oral, multi-targeted kinase inhibitor, which has been approved for treatment of imatinib-resistant gastrointestinal stromal tumor and renal cell carcinoma. Additionally, sunitinib is in clinical trials for CML and myelodysplastic syndromes. Sunitinib is a potent inhibitor of receptor tyrosine kinase c-KIT [35], and the serine/threonine protein kinase PRKAA1 (AMPK1α) and CAMK2 [36]. Overall, we could show that our optimised elution method brought a universal improvement in elution efficiency with two different drug-coupling strategies and two different kinase inhibitors.

3. Materials and methods

3.1. Chemicals

All chemicals used were of analytical grade, unless stated otherwise and obtained from commercial suppliers.

3.2. Biological material

K562 and HEL cells were obtained from DSMZ (Deutsche Sammlung von Mikroorganismen und Zellkulturen). Antibodies used were rabbit polyclonal anti-DDR1, anti-BTK (E9) and anti-KIT (C-19) (Santa Cruz Biotechnology, Santa Cruz, CA); and anti-ABL (21–63) (generated in house).

3.3. Compounds and immobilization

Dasatinib and sunitinib were purchased from Selleck Biochem (Houston, Texas Area). c-dasatinib was synthesized by WuXi PharmaTech (Shanghai, China) [21], and c-sunitinib was obtained from Indus Biosciences Private Limited (Hyderabad, India) through Gateway Pharma (Freeland, UK). Compounds were immobilized on NHS-activated Sepharose 4 Fast low (Amersham Biosciences, Amersham, UK). Beads were washed with dimethyl sulfoxide (DMSO) and incubated overnight with 1 mM compound and 100 mM triethylamine (TEA) at room temperature (RT) with constant agitation. After incubation, the supernatant was analyzed by high-performance liquid chromatography mass spectrometry (HPLCMS) in order to determine whether the compound was completely immobilized. Unreacted functional groups were subsequently blocked with 0.8 M ethanolamine for at least 8 h at RT, washed with DMSO and either stored at 4 °C in isopropyl alcohol or used immediately for affinity chromatography. For the biotinylated drug experiments, c-dasatinib was incubated with biotin amidohexanoyl-6-aminohexanoic acid *N*-hydroxysuccinimide ester (biotin-XX-NHS, Sigma–Aldrich, St. Louis, MO) in the presence of TEA overnight at RT with constant agitation. The supernatant was then analyzed by HPLC-MS for residual reagents and the reaction yield. Dasatinib coupled to biotin was incubated with UltraLink immobilized streptavidin plus beads (Pierce, Rockford, IL) on a roto-shaker for 30 min at 4 °C and used for affinity chromatography.

3.4. Affinity purification

The same affinity purification protocol was used for c-dasatinib, c-sunitinib and c-dasatinib-XX-biotin. K562 and HEL cell lysates were prepared using a lysis buffer comprised of 50 mM Tris–HCl (pH 7.5), 100 mM NaCl, 0.2% NP-40, 5% glycerol, 1.5 mM $MgCl_2$, 25 mM NaF, 1 mM Na_3VO_4, 1 mM phenylmethylsulfonyl fluoride (PMSF), 1 mM dithiothreitol (DTT), 10 μg/mL *N*-alpha-tosyl-L-lysinyl-chloromethylketone (TLCK), 1 μg/mL leupeptin, 1 μg/mL aprotinin, and 10 μg/mL soybean trypsin inhibitor. In order to minimise sample variability, cell lysates were prepared in large batches, aliquoted and stored at −80 °C until required. Before application to the pre-equilibrated affinity matrices, cell suspensions were clarified by centrifugation. Lysates (5 and 10 mg total protein for K562 and HEL, respectively) were incubated with drug-

coupled affinity matrices for 2 h at 4 °C. After a brief centrifugation, the lysates were transferred to 2 mL Bio-Spin disposable chromatography columns (BioRad, Hercules, CA). Columns were washed with lysis buffer and then with 50 mM HEPES–NaOH buffer (pH 7.5) supplemented with 0.5 mM EDTA (pH 8.0) and 100 mM NaCl. Retained proteins were eluted in several ways: (i) immediate elution without incubation; (ii) heat denaturation by boiling (B) at 100 °C, either for 5 min or 1 h; and (iii) incubation for 1 h at 57 °C or 60 °C. As elution agents, the following freshly-prepared stocks were used: (i) 250 μL 100 mM FA; (ii) 300 μL 6 M urea; (iii) 300 μL 1 M NaCl; (iv) 300 μL 25% CH_3CN (acetonitrile, ACN); (v) 300 μL 50% CH_3CN; (vi) 250 μL 3 M urea, 50 mM FA (U/FA); (vii) 250 μL 0.5M NaCl, 50 mM FA (NaCl/FA); (viii) 250 μL 50% CH_3CN, 50 mM FA (ACN/FA); (ix) HEPES buffer; and (x) 30 μL sodium dodecyl sulfate (SDS) sample buffer (Laemmli buffer) combined with boiling for 4 min. In some cases, a double elution procedure was applied (denoted as .2). After elution with a given agent (*e.g.*, FA or U/FA), the eluate was collected in a glass vial and re-loaded onto the drug-affinity matrix and the flow-through collected a second time. On any occasion where FA was used either as a single agent or in combination with other components, proteins were eluted into a glass vial containing either 62.5 μL (FA elution alone) or 31.25 μL (combinations with FA) 1 M triethylammonium bicarbonate (TEAB) to neutralize the acidic eluate. Whenever FA was not used, retained proteins were eluted directly into a glass vial using a higher volume of eluting agent to maintain the same final volume for all eluates throughout the experiments. For ACN or ACN/FA and ACN/FA.2, eluted proteins were lyophilised by vacuum centrifugation and reconstituted in 100 mM TEAB. After elution of the proteins, the same sample preparation protocols were used throughout. An aliquot of each eluate (100 μL) was removed for immunoblot analysis and denatured by boiling for 4 min with Laemmli buffer. In an initial screen with c-dasatinib where four selected elution methods were compared to a standard FA protocol, one biological replicate of each was analysed as technical duplicates. For the U/FA.2 elution pulldowns with c-dasatinib and c-sunitinib, five and two biological replicates were analysed, respectively. Experiments conducted with c-dasatinib-XX-biotin consisted of four biological replicates.

3.5. Immunoblot analysis

For the western blot experiments, eluates containing Laemmli buffer were separated by 1D SDS-PAGE on a 7% polyacrylamide gel. Blotting was performed for 1 h onto a nitrocellulose transfer membrane (Protran BA 85, 0.45 μm). After blocking with either 5% non-fat dry milk or 3% BSA in TBS/Tween, the membrane was incubated with the primary antibody overnight at 4 °C and then for 1 h at RT with the secondary antibody. The signal was detected using radiographic films after incubation with chemi-luminescence detection reagent (ECL normal or ECL plus, GE Healthcare Bio-Sciences, Uppsala, Sweden). For the dot blot experiments, eluates containing Laemmli buffer were spotted onto a nitrocellulose membrane using a Bio-Dot apparatus (Biorad, Hercules, CA) as previously described [37]. The membrane was dried, rehydrated and analyzed by immune staining. Two 1:5 serial dilutions of the eluates were used throughout to extend the dynamic range of the immunoblot signal. This was essential to observe subtle differences in intensity.

3.6. Solution tryptic digestion of eluted proteins and sample preparation for liquid chromatography mass spectrometry

Based on the immunoblot experiments, non-acidic eluates were not analysed by LCMS. The TEAB-neutralized acidic eluates, however, were reduced with 500 mM DTT at 56 °C for 1 h (final concentration DTT approximately 10 mM) and alkylated with 1 M iodoacetamide for 30 min at room temperature in the dark (final concentration iodoacetamide approximately 55 mM). Depending on the preceding elution procedure and prior to digestion with trypsin, samples were diluted with 500 mM TEAB to a concentration of 250 mM NaCl or 1.5 M urea. All final volumes of the various samples were kept constant throughout. Digestion was performed with sequencing grade modified porcine trypsin (Promega, Madison, WI) overnight at 37 °C. Eluates were desalted using stage tips [38] (3 × 5% of the digest volume per drug pulldown), concentrated in a vacuum centrifuge (Eppendorf, Hamburg, Germany) to approximately 2 μL and then reconstituted with 24 μL 5% FA. All samples were analysed by LCMS as technical replicates.

3.7. Liquid chromatography mass spectrometry

Mass spectrometry was performed on an linear trap quadrupole (LTQ) Orbitrap Velos mass spectrometer (ThermoFisher Scientific, Waltham, MA) using Xcalibur version 2.1.0 SP1.1160. The instrument was coupled to an Agilent 1200HPLC nanoflow systems (dual pump with one precolumn and one analytical column) (Agilent Biotechnologies, Palo Alto, CA) via a nanoelectrospray ion source using a liquid junction (Proxeon, Odense, Denmark). Solvents for LCMS separation of the digested samples were as follows: solvent A consisted of 0.4% FA in water and solvent B consisted of 0.4% FA in 70% methanol and 20% isopropanol. Eight microlitres of the tryptic peptide mixture were automatically loaded from a thermostatted microautosampler onto a trap column (Zorbax 300SB-C18 5 μm, 5 × 0.3 mm, Agilent Biotechnologies, Palo Alto, CA) with a binary pump at a flow rate of 45 μL/min. TFA (0.1%) was used for loading and washing the precolumn. After washing, the peptides were eluted by back-flushing onto a 16 cm fused silica analytical column with an inner diameter of 50 μm packed with C18 reversed phase material (ReproSil-Pur 120C18-AQ, 3 μm, Dr. Maisch GmbH, Ammerbuch-Entringen, Germany). The peptides were eluted from the analytical column with a 27 min gradient ranging from 3 to 30% solvent B, followed by a 25 min gradient from 30 to 70% solvent B and, finally, a 7 min gradient from 70 to 100% solvent B at a constant flow rate of 100 nL/min [39]. The analyses were performed in a data-dependent acquisition mode and dynamic exclusion for selected ions was 60 s. A top 15 collision-induced dissociation (CID) method was used, and a single lock mass at *m/z* 445.120024 [$Si(CH_3)_2O)_6$] [40] was employed. Maximal ion accumulation time allowed in the CID mode was 50 ms for MS^n in the LTQ and 500 ms in the C-trap. Automatic gain control was used to prevent overfilling of the ion traps and was set to 5000 in the MS^n mode for the LTQ and 10^6 ions for a full FTMS scan. Intact peptides were detected 60,000 resolution at *m/z* 400 [39].

3.8. Data analysis

The acquired raw MS data files were processed with msconvert (ProteoWizard Library v2.1.2708) and converted into Mascot generic format (.mgf) files. The resultant peak lists were searched against the human Swiss-Prot database version v2011.06_20110609 or v2011.12_20111220 (35683 and 35879 sequences, respectively, including isoforms as obtained from varsplic.pl) with the search engines Mascot (v2.3.02, MatrixScience, London, U.K.) and Phenyx (v2.5.14, GeneBio, Geneva, Switzerland). Submission to the search engines was via a Perl script that performs an initial search with relatively broad mass tolerances (Mascot only) on both the precursor and fragment ions (±10 ppm and ±0.6 Da, respectively). High-confidence peptide identifications were used to calculate independent linear transformations for both precursor and fragment ion masses that

would minimize the mean square deviation of measured mass from theoretical. These recalibrating transformations were applied to all precursor and fragment ions prior to a second search with narrower mass tolerances (±4 ppm and ±0.3 Da). One missed tryptic cleavage site was allowed. Carbamidomethyl cysteine and oxidized methionine were set as fixed and variable modifications, respectively. To validate the proteins, Mascot and Phenyx output files were processed by internal parsers. Proteins with ≥2 unique peptides above a score T1, or with a single peptide above a score T2, were selected as unambiguous identifications. For validated proteins fulfilling either the T1 or T2 criteria, any additional peptides with a score >T3 were also accepted. For Mascot and Phenyx, T1, T2, and T3 peptide scores were 16, 40, and 10; and 5.5, 9.5, and 3.5, respectively (P-value $<10^{-3}$). For each data set the validated peptides retrieved by the two algorithms were merged, any spectral conflicts discarded and proteins grouped according to shared peptides. A false discovery rate (FDR) of <1% and <0.1% (including the peptides exported with lower scores) was determined for proteins and peptides by applying the same procedure against a reversed database. To compare the efficiency of the elution protocols, the distributed normalized spectral abundance factors (dNSAF) [41] were used as a measure of protein abundance.

$$\mathrm{dSAF}_i = \frac{1}{L_i}\left(\mathrm{uSC} + \sum_{k=1}^{N_{\mathrm{spep}}(i)} \frac{\mathrm{uSC}_i}{\sum_{l=1}^{N_{\mathrm{sprot}}(k)} \mathrm{uSC}_l} \mathrm{sSC}_{i,k}\right) \quad (1)$$

$$\mathrm{dNSAF} = \frac{\mathrm{dNSAF}_i}{\sum_{l=1}^{N} \mathrm{dNSAF}_l} \quad (2)$$

Briefly, the distributed spectral abundance factor (dSAF) of protein i is the weighted sum of the spectral counts divided by protein length. The weight of unique spectral counts (uSC) is 1, whereas the weight of spectra for k-th shared peptide ($\mathrm{sSC}_{i,k}, k = 1, 2, .. N_{\mathrm{spep}}(i)$) is the ratio of unique spectral counts of protein i and the sum of all unique spectral counts for $N_{\mathrm{sprot}}(k)$ proteins that share k-th peptide. Finally, dSAF is normalized to the total sum of dSAFs in the specific LCMS analysis to obtain dNSAF (2). For each drug, the effect of each elution protocol on the abundance of the two protein groups was assessed: known targets and interactors ('T'), and known contaminants ('C': spectrin, actin, myosin, vimentin, haemoglobin subunits, histone and ribosomal proteins, heterogeneous ribonuclear proteins, POTE ankyrin domain family members). Specifically, the following generalized linear regression model was applied to dNSAF data:

$$A_{i,j} = a_0 + a_i + p_{G(i),P(j)} + q_{i,P(j)} + b_{B(j)} + e_j + d_{i,B(j)}, \quad (3)$$

$$\log(\mathrm{dNSAF}_{i,j}) \propto \mathrm{Normal}(A_{i,j}), \quad (4)$$

$$I_{i,j} \propto \mathrm{Bernoulli}\left(\mathrm{logit}^{-1}(\alpha A_{i,j} + \beta)\right), \quad (5)$$

where $i = 1, 2. .. N$ and $j = 1, 2,... M$ specify the protein and LCMS analysis, respectively, and $A_{i,j}$ is the abundance of i-th protein in the j-th experiment. $A_{i,j}$ takes into account the following factors: a_0—the average protein abundance; $a_0 + a_i$—the average abundance of i-th protein; $p_{G(i),\,P(j)}$—the average effect of the elution protocol ($P(j)$) on a given group of proteins ($G(i)$, either targets or contaminants); $q_{i,P(j)}$—the protocol effect on the individual protein; e_j—the normalization term for the j-th LCMS analysis; $b_{B(j)}$ and $d_{i,B(j)}$ account for the global and protein-specific effects of the $B(j)$-th batch of LCMS analyses. The equation (4) links the observed $\mathrm{dNSAF}_{i,j}$ to $A_{i,j}$. Bernoulli-logit model (5) is used to properly account for missing data: protein identification ($I_{i,j} = 1$) or absence ($I_{i,j} = 0$) in a given experiment is linked to inferred abundance $A_{i,j}$, where parameters α and β are learned from the data.

The model (3)–(5) enables an assessment of how a given protocol affects the abundance of specific protein groups (either targets or contaminants) and individual proteins. At the same time, these protocol-specific effects are decoupled from batch-specific and individual LCMS data variations. The Bayesian methodology was adopted and the model (3)–(5) was fit to the experimental data using STAN [42] to obtain the posterior distributions for all the model parameters. The posterior distributions for protein group-specific protocol effects ($p_{J,G}$) were used to estimate the overall protocol efficiencies:

$$\mathrm{Eff}(J) = (p_{J,T} - p_{J,C}) - (p_{0,T} - p_{0,C}). \quad (6)$$

That is, Eff(J) reports how much the target proteins (T) are enriched over the contaminants (C) when using protocol J in comparison to the 0-th reference protocol (U/FA). It follows from (6) that Eff(J) is positive for more efficient protocols, and one-sided P-value

$$P(\mathrm{Eff}(J) \le 0) \quad (7)$$

provides the statistical significance of this hypothesis.

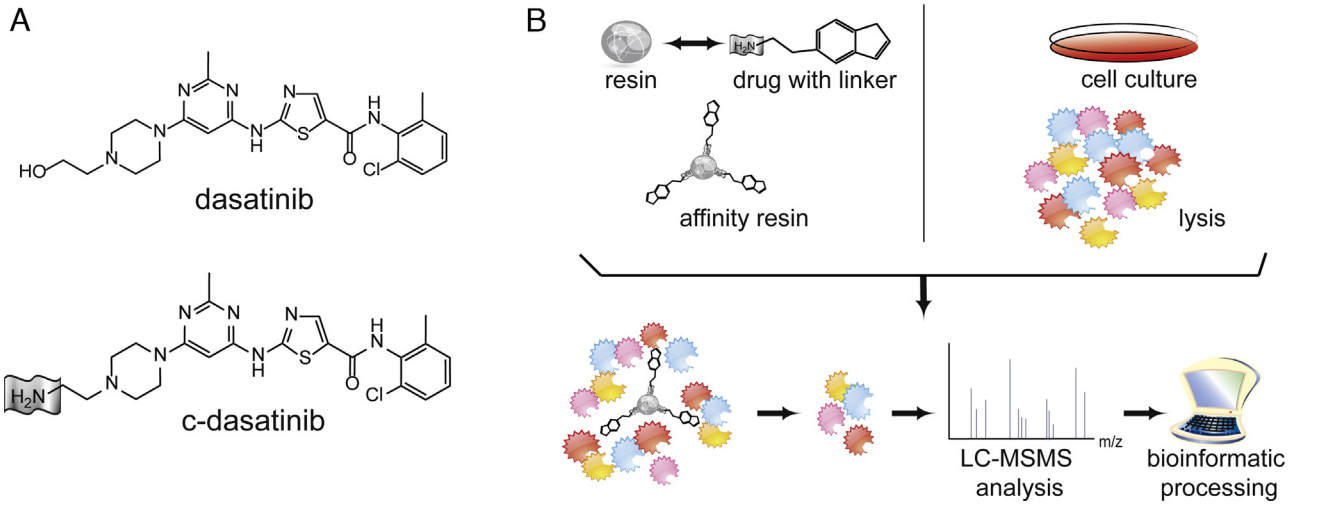

Fig. 1. Overview of the experimental approach. (A) Chemical structure of dasatinib and c-dasatinib. The latter is the chemically-modified version of dasatinib that can be coupled to sepharose beads via a linker. (B) The overall workflow of a chemical proteomic experiment.

4. Results and discussion

4.1. Combining formic acid with denaturing reagents improves detection of BCR-ABL, DDR1 and BTK by immunoblotting.

The dasatinib analog (Fig. 1A) was coupled to NHS-sepharose beads and the resultant drug affinity matrix was incubated with cell extracts from the chronic myelogenous leukemia (CML) cell line K562 (5 mg protein per pulldown) (Fig. 1B). A number of different elution reagents and/or conditions were used: (i) 100 mM formic acid (FA); (ii) 6 M urea (U) [43]; (iii) 1 M NaCl; (iv) 25% acetonitrile (ACN) [44,45]; (v) 50% ACN [44]; (vi) 3 M urea, 50 mM FA (U/FA); (vii) 0.5 M NaCl, 50 mM FA (NaCl/FA); (viii) 50% ACN, 50 mM FA (ACN/FA); (ix) HEPES buffer; and (x) 4 × SDS sample buffer (Laemmli buffer). The latter is the traditional method for gel-based approaches and acts as a control for evaluating the protein targets of a drug by immunoblot analyses. Elution with 100 mM FA (no incubation of the proteins on the affinity matrices) is our previously-established, standard elution procedure for gel-free drug pull-down experiments [23]. All elution protocols assessed were compared to this 'standard protocol'. Reagents were evaluated at RT or 100 °C (B) for 4 min or 1 h. A 1 h incubation at 57 °C and 60 °C was also assessed for the urea and ACN elutions, respectively. It has been previously suggested that the efficiency of protein elution may be improved when incubating at higher temperatures [44]. In the early stages of the study, one goal was to establish a reproducible immunoblotting method that would enable a rapid comparison between selected elution methods. The dot blot approach allows the direct application of a sample onto a membrane without prior separation by electrophoresis. Furthermore, proteins are transferred by microfiltration. This eliminates any variability caused by the transfer of a protein from a gel. Based on previous experiments with dasatinib, three antibodies (c-ABL, DDR1 and BTK) were selected. These proteins are *bona fide* dasatinib targets [6,21,31] and belong to different kinase classes: non-receptor kinases from ABL and TEC family (c-ABL and BTK, respectively) and receptor tyrosine kinase (DDR1). The differences between the elution methods were assessed by direct comparison to the standard elution procedure (Fig. 2). When used as single agents (Fig. 2A), both 6 M urea (lane 3) and 1 M NaCl (lane 7) gave a weaker signal for both c-ABL and DDR1 than the standard FA elution (lane 2). When the samples were boiled (B) for 4 min,

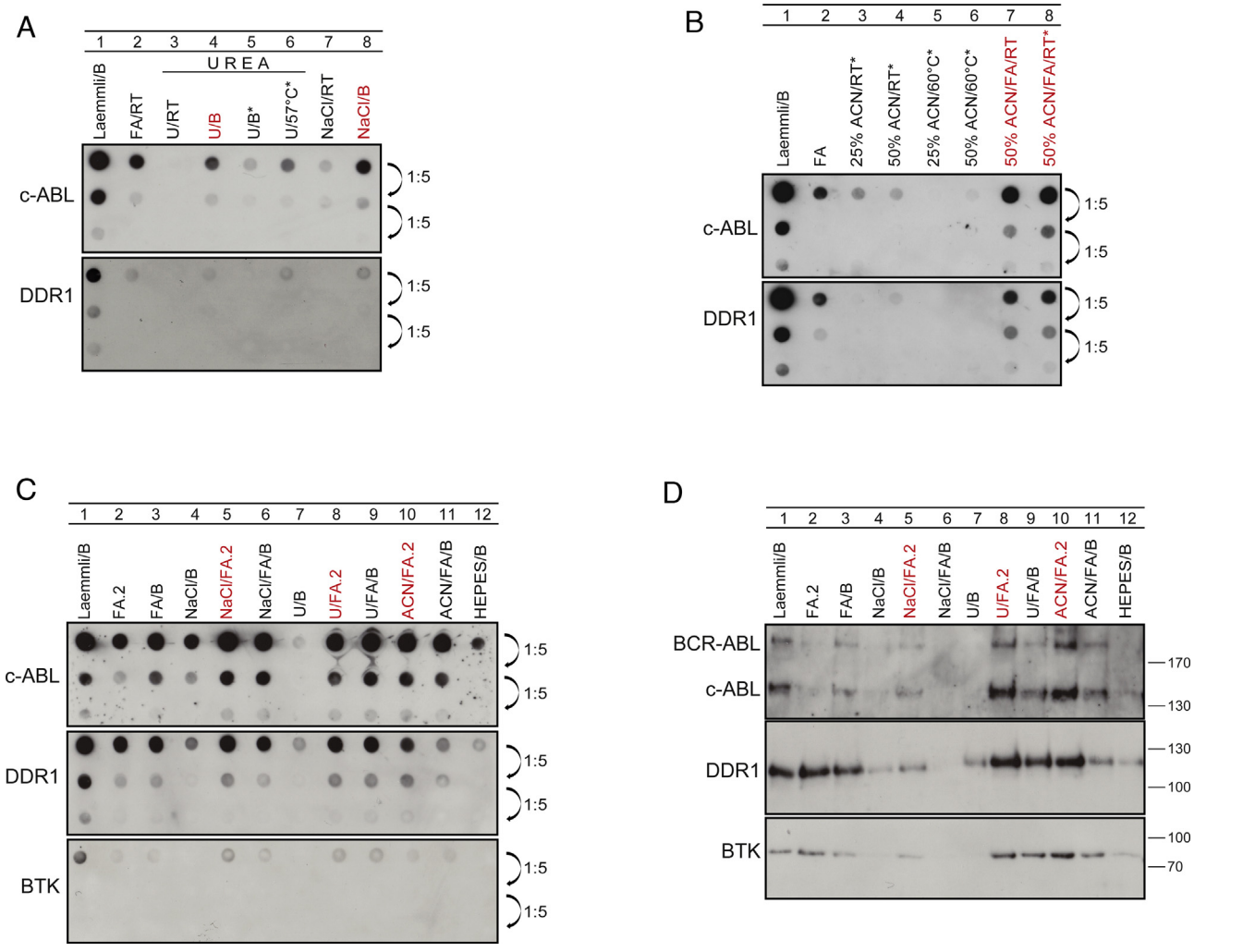

Fig. 2. Combination of formic acid with denaturing reagents improves elution efficiency for BCR-ABL, DDR1 and BTK. (A) Anti-ABL and anti-DDR1 dot blots of pulldowns eluted with urea and NaCl. Five-fold serial dilutions from each eluate were also loaded. B, boiled; *, 1 h incubation of the elution agent on the column. (B) Anti-ABL and anti-DDR1 dot blots of pulldowns eluted with different concentrations of acetonitrile and combined with formic acid. Five-fold serial dilutions from each eluate were also loaded. *, 1 h incubation of the elution agent on the column. (C) Anti-ABL, anti-DDR1 and anti-BTK dot blots of pulldowns eluted with various elution agents and procedures. Double application of the eluate to the column is denoted as .2. Five-fold serial dilutions from each eluate were also loaded. B, boiling. (D) Anti-ABL, anti-DDR1 and anti-BTK western blots of pulldowns eluted with same agents and conditions as in (C), B, boiling. (For interpretation of the references to color in the text, the reader is referred to the web version of this article.)

however, the results were in the same range as the standard protocol or even slightly improved (lanes 4 and 8, highlighted in red). A longer incubation time of 1 h (indicated by asterisks) with urea at 57 °C (lane 6) or 100 °C (lane 5) did not lead to any visible improvement in elution efficiency. The ACN elution was also weak (Fig. 2B). Even after a 1 h incubation at RT (lanes 3 and 4) or 60 °C (lanes 5 and 6), ACN as a single elution agent only resulted in a faint to no signal. Nevertheless, when ACN was combined with FA (lanes 7 and 8, highlighted in red), signal intensity was markedly improved. Regardless of whether the proteins were immediately eluted from the drug affinity matrix or after a 1 h incubation period, the 50% ACN/50 mM FA combination at RT enhanced the elution and immunoblot efficiency to an extent comparable to the Laemmli control (lane 1). This experimental condition was also notably improved over the standard FA elution (lane 2).

As the combination of ACN with FA at RT led to a significant improvement in signal intensity, our next step was to evaluate the effect on protein elution from the drug affinity matrix when all of the selected reagents were combined with FA. Furthermore, we reasoned that more proteins could be retrieved if the eluate was applied to the column twice. Regardless of the reagent chosen, the eluate was collected, applied to the column a second time, and the eluate again collected in a glass vial (denoted as .2 in all ensuing text). At this point too, an improvement in elution efficiency by boiling the samples was not excluded. Thus, to assess whether boiling of the samples alone is sufficient to potentiate elution efficiency, HEPES buffer was included in the panel of elution agents. Dot and western blot analyses of the various eluates for c-ABL, DDR1 and BTK (Fig. 2C and D) showed that the elution efficiency was markedly enhanced for all three targets when denaturing agents were combined with formic acid. A double elution with 50 mM FA combined with either 0.5 M NaCl (NaCl/FA.2) (Fig. 2C, lane 5, highlighted in red); 3 M urea (U/FA.2) (lane 8, highlighted in red); and 50% ACN (ACN/FA.2) (lane 10, highlighted in red) all showed an increase in elution efficiency over the standard procedure where formic acid was used as a single agent and at a higher concentration of 100 mM (lane 2). Also, it was observed that in most cases boiling of the samples did not lead to enhancement of the signal intensity (lanes 6, 9, 11, 12). In some instances, quite the contrary a weaker signal was apparent compared to the counterparts that were not boiled (see lane 11 compared to lane 10). Furthermore, boiling of the HEPES eluate (lane 12) did not result in increased protein recovery. Thus, we concluded that the combination of a selection of agents with FA is

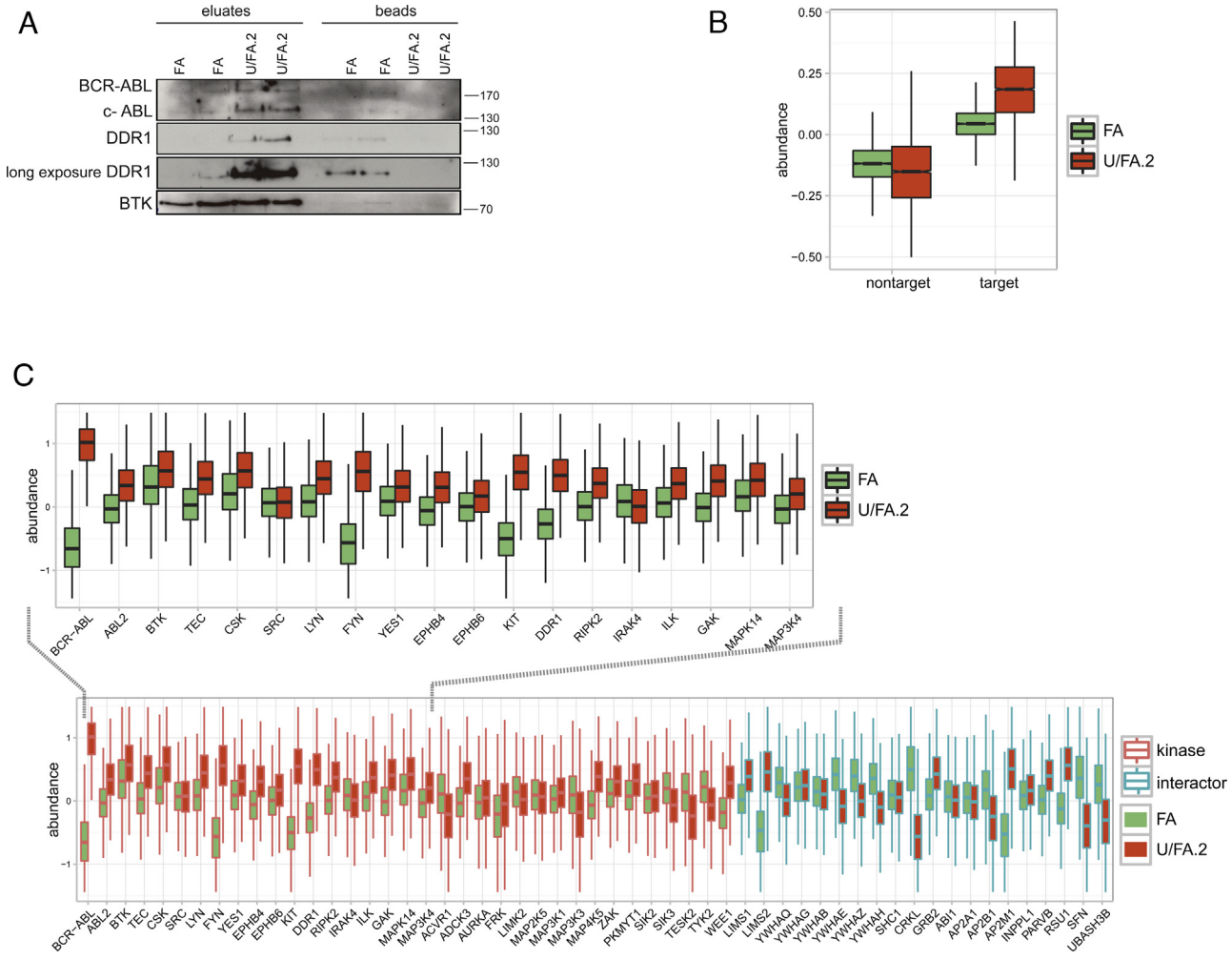

Fig. 3. Formic acid/urea double elution improved the identification of dasatinib targets by gel-free liquid chromatography mass spectrometry. (A) Anti-ABL, anti-DDR1 and anti-BTK western blots of pulldowns eluted with either FA or U/FA.2, plus the beads sequentially eluted with Laemmli buffer. (B) Comparison of the overall abundance between FA and U/FA.2. (C) The majority of the cognate kinase targets of dasatinib are more abundant with U/FA.2 than FA alone. This is particularly noticeable for the main target of dasatinib, BCR-ABL. An integrated plot showing differences in protein abundance between the FA alone and the U/FA.2 elution methods. Kinases and kinase-interacting proteins are indicated in the red and blue box plots, respectively. Recovery of all major kinase targets was improved with U/FA.2, whilst the majority of the kinase-interacting proteins are less abundant. Five biological replicates were analysed (two technical replicates each). (For interpretation of the references to color in this figure legend, the reader is referred to the web version of this article.)

sufficient for signal improvement, and this holds true for all three selected targets of dasatinib: ABL, receptor tyrosine kinase DDR1 and the TEC kinase family member, BTK.

BCR-ABL is the main target of dasatinib. Similarly, c-ABL is also one of the primary targets. As shown in Fig. 2D, both proteins were recognized by the anti-ABL antibody as evidenced by bands detected for ABL and BCR-ABL at approximately 140 kDa and 210 kDa, respectively. As mentioned previously, one of the main issues with the current 100 mM FA standard elution method is the inability to retrieve ABL proteins with high efficiency from the dasatinib-coupled affinity matrix. This was already apparent from the dot blot, and is particularly noticeable in the first 5-fold dilution series (Fig. 2C, upper panel, lane 2). Excluding HEPES (lane 12) and U/B (lane 7), the recovery with FA was lower than all the other elution methods assessed. Even more striking is this difference on the western blot (Fig. 2D). Here the signal in the FA eluate is almost completely absent for both BCR-ABL and ABL (upper panel, lane 2). Conversely, the recovery of these proteins with U/FA.2 (lane 8, highlighted in red) and ACN/FA.2 (lane 10, highlighted in red) was even higher than that observed with Laemmli buffer (lane 1). The difference was not as pronounced with the two other dasatinib targets, DDR1 and BTK. Nevertheless, an improvement was still observed when the same set of elution procedures was used; namely U/FA.2 (middle and lower panels, lane 8, highlighted in red), U/FA/B (lane 9), ACN/FA.2 (lane 10, highlighted in red) and ACN/FA/B (lane 11). In addition, NaCl/FA.2 (lane 5, highlighted in red) also showed a slight improvement in elution efficiency. This was particularly noticeable for BCR-ABL and ABL. An overall comparison of these data showed that on the immunoblot level, an improvement in the recovery of selected dasatinib targets was achieved in all instances when formic acid was combined with a denaturing reagent.

4.2. Combining formic acid with denaturing reagents improved detection of dasatinib targets by mass spectrometry.

We next asked the question: whether improvement in target recovery as observed from the immunoblot analyses would also translate into a higher quality data set by LCMS. Therefore, the most promising elution methods as determined by immunoblot, *i.e.*, FA.2, U/FA.2, NaCl/FA.2, and ACN/FA.2 were screened by LCMS (Supplementary Table S1). The spectral count values were used as an indicator of target importance; as this represents a combination of target affinity and abundance [46]. When the average spectral counts (from two technical replicates) of selected elution methods were compared for relevant dasatinib targets, we observed that FA.2 did not show an increase in elution efficiency. This led to the conclusion that the double elution alone is not sufficient to improve the standard method. Rather, it is the joint effect of the double elution together with the appropriate combination of elution reagents. When the other elution methods were compared to the standard FA protocol, the most striking difference was observed for BCR-ABL. An almost four-fold increase in average spectral counts was apparent for the U/FA.2 and ACN/FA.2 elutions (from 15 spectral counts with FA alone; to 55 and 61.5, respectively, for the alternate elution methods). Apart from the substantial increase in the elution efficiency of ABL kinases, the data obtained from the LCMS screen of the proteins eluted with U/FA.2 and ACN/FA.2 appeared to be comparable to the standard method. Nonetheless, both elution methods displayed a noticeable improvement in the immunoblot experiments (Fig. 2C and D). The U/FA.2 and ACN/FA.2 immunoblot and LCMS data were quite similar; however, due to the simplicity of the sample preparation only the U/FA.2 method was investigated further (see below). To confirm that the observed increase in cognate target recovery was due to improved elution and not as a consequence of other factors such as downstream sample loss, Laemmli buffer was added to the beads after the proteins had been eluted. The beads were boiled for 5 min and loaded onto a gel together with the eluates. For all three of the targets (ABL, DDR1 and BTK) assessed by immunoblot, a clear improvement in elution with U/FA.2 compared to the standard FA was evident. In support of this observation, residual protein on the beads was not apparent for U/FA.2 (Fig. 3A). Conversely, some protein was retained on the beads when FA alone was used.

To assess both the robustness and consistency of the new method, five new cycles of FA and U/FA.2 elution experiments were conducted and analysed by LCMS (Fig. 3B and C, Supplementary Table S2). Compared to FA alone (Fig. 3B, light green), elution with U/FA.2 (red) resulted in higher target recovery. The list of dasatinib targets consisted of all validated protein kinase targets and indirect binders of the drug, *i.e.*, the interactors of target kinases [6,21,29,47–50]. When specifically assessing the kinase targets of dasatinib, the target enrichment was even more evident (Fig. 3C). The majority of the kinases were more abundant in U/FA.2 compared to the standard FA eluates. Contingent on previously-published data using gel-based approaches [21,33,48], the dasatinib targets identified with the U/FA.2 elution accurately reflected the expected distribution of primary and secondary interactors. In addition to the dramatic difference observed with BCR-ABL, ABL2, kinases from the SRC family (LYN, FYN, YES1 and c-SRC), and the negative regulator c-SRC kinase (CSK) showed improvement. The TEC family kinases (BTK and TEC) are prominent interactors of dasatinib [6] and were also eluted more efficiently. Likewise, the receptor tyrosine kinases DDR1, KIT, EPHB4 and EPHB6 and the serine–threonine kinases (GAK, MAPK14, MAP3K4) were also identified with higher spectral count abundances. RIPK2 was also eluted with higher efficiency. This kinase is a member of the receptor-interacting protein (RIP) family of serine/threonine protein kinases, and is a known target of dasatinib that has not been reported with other ABL kinase inhibitors (*e.g.,* imatinib, nilotinib or ponatinib) [51].

One of the drawbacks of chemical proteomics is that it is often difficult to distinguish direct from indirect targets. With the U/FA.2 elution method, however, the contribution from several non-kinase proteins was reduced (Fig. 3C), *e.g.*, 14-3-3 proteins, CRKL, UBASH3B, *etc.* This apparent reduction (as determined by spectral counts) may reflect a decrease in MS sampling for these proteins due to the concurrent increase in sampling of the now more efficiently eluted true interactors. On the other hand, the integrin-linked kinase ILK together with the non-kinase interaction partners LIMS1, LIMS2, PARVB and RSU1 were consistently observed with notably improved recovery (Fig. 3C). These molecules form a very robust IPP complex (ILK, PINCH and parvin complex) [52] and thus, do not follow the same trend as other non-kinase proteins. Rather, these too were eluted more efficiently with U/FA.2. Based on our spectral counting approach, the data generated from the U/FA.2 elution method suggested that this particular combination of reagents may aid in refining the distinction between direct and indirect interacting proteins.

4.3. U/FA.2 is an elution method of choice for biotinylated compounds

Although the widely-applied chemical immobilization of a bioactive small molecule on an inert matrix has proven highly-successful in many chemical proteomic studies; there are a few drawbacks. Synthesising a coupleable analog of a compound is not always straightforward. An alternative is to utilise the well-established biotin/avidin affinity purification system. Here, modification of a small molecule with a biotin tag enables the non-covalent capture of drug-protein complexes by (strept) avidin.

Previous observations from our group (data not shown) revealed that the standard formic acid-based elution method did not result in sufficient recovery of proteins when using biotinylated compounds as the bait; thereby precluding a successful analysis of such drug target interactions by gel-free LCMS. We therefore evaluated, if the elution method optimized in the preceding section would be more successful with respect to the identification of proteins that are enriched with a biotinylated small molecule. To answer this question, dasatinib was biotinylated (Fig. 4A), attached to streptavidin beads, incubated with K562 cell lysates (5 mg total protein per experiment) and eluted using the various methods described earlier (urea, NaCl, ACN), with or without boiling, in combination with formic acid and with a double elution. Initial dot blot analyses with an ABL-specific antibody confirmed the feasibility of this molecule as a chemical proteomic probe as the elution with Laemmli buffer (positive control) readily recovered ABL proteins (Fig. 4B, lane 1). Strikingly, but consistent with previous observations [23], no signal was evident following elution with 100 mM formic acid (Fig. 4B, upper panel, lane 2). The complete absence of the main target of dasatinib was also confirmed by western blot (Fig. 4B, lower panel, lane 2). In contrast, the double elution with urea combined with formic acid produced an excellent immunoblot signal (Fig. 4B, upper panel, lane 8, highlighted in red; lower panel, lane 4, highlighted in red) which was comparable to that obtained with Laemmli buffer (lane 1). LCMS analysis of these eluates (Supplementary Table S3) strengthened the notion that U/FA.2 is the method of choice to elute target proteins of biotin-coupled drugs (Fig. 4C). Target

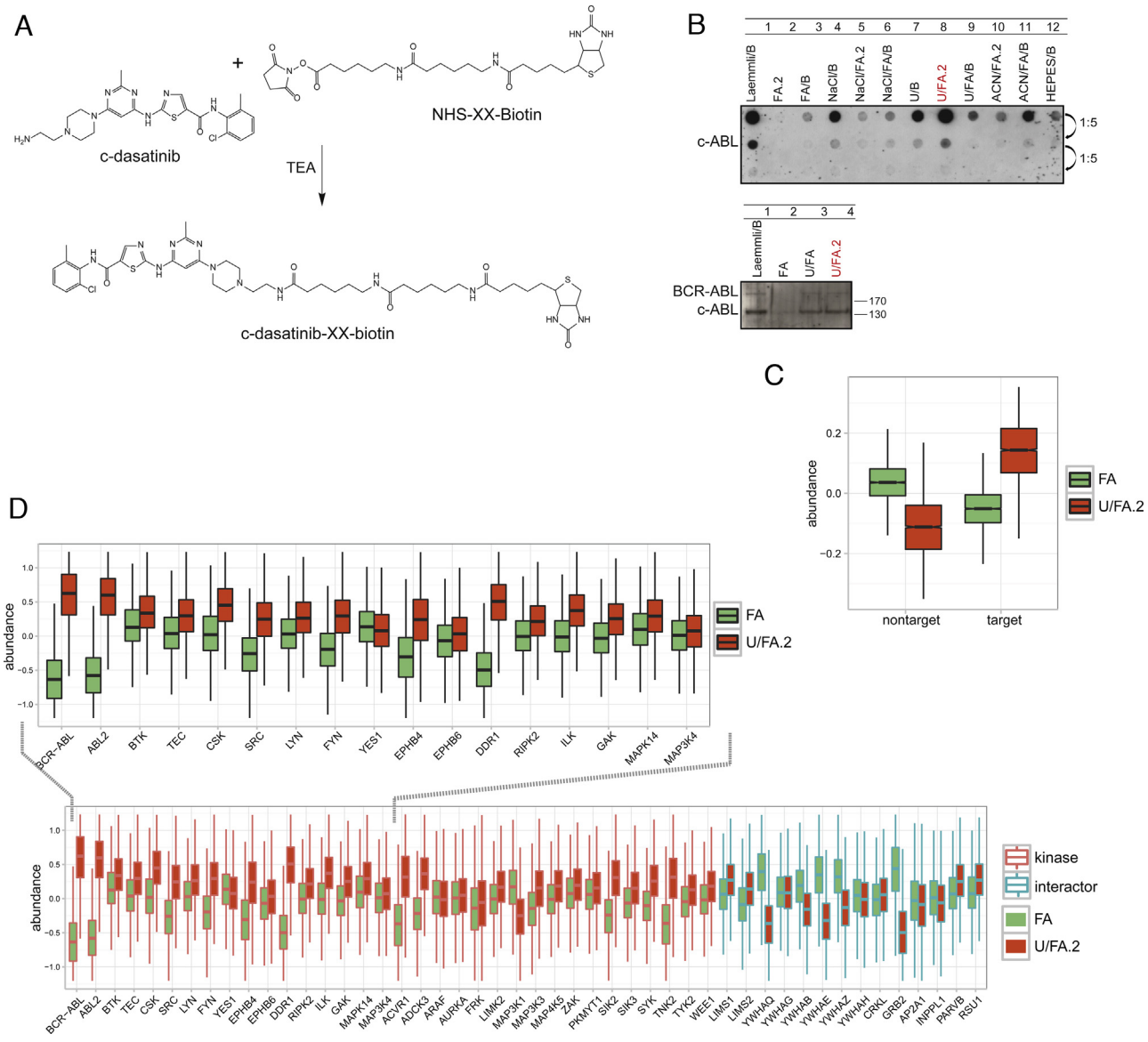

Fig. 4. Double elution with formic acid combined with urea improved the elution of proteins bound to biotinylated dasatinib. (A) Reaction to produce the biotinylated version of c-dasatinib for coupling to streptavidin beads. (B) Upper panel: anti-ABL dot blot of the pulldowns that were eluted with the various elution agents and procedures that were used in the c-dasatinib pulldowns. Five-fold serial dilutions from each eluate were also loaded. Double application of the eluate to the column is denoted as .2. B, boiled. Lower panel: anti-ABL western blot of pulldowns performed with the positive control (Laemmli), standard (FA) and U/FA (both single and double elution). Immunoblot signal for ABL is completely absent when the standard elution with 100 mM FA was used, whilst the signal is strong in the U/FA and U/FA.2 pulldowns. (C) Comparison of overall abundances between FA and U/FA.2. Four biological replicates were analysed (two technical replicates each). (D) The majority of cognate kinase targets of dasatinib are more abundant in U/FA.2 than FA. BCR-ABL was completely absent in the FA pulldowns, but had the highest recovery compared to other kinase targets when U/FA.2 was used as the elution method. An integrated plot showing differences in abundances between the FA and U/FA.2 elution methods is shown. Kinases and kinase-interacting proteins are indicated in the red and blue box plots, respectively. Recovery of all major kinase targets was improved with U/FA.2, whilst the majority of the kinase-interacting proteins (excluding the IPP complex) are less abundant. (For interpretation of the references to color in this figure legend, the reader is referred to the web version of this article.)

protein abundance was highly enriched for U/FA.2 (red) compared to FA alone (green). At the same time, non-target protein abundance was reduced. In addition, the ratio between target and non-target proteins was unfavorable for FA alone; whereas for the U/FA.2 elution, proteins that specifically interact with dasatinib were recovered with considerably higher abundance. This was even more apparent when specific dasatinib kinase targets were compared (Fig. 4D). In the FA pulldowns (green), BCR-ABL was completely absent, but was identified with high abundance by U/FA.2 elution (red). All other major targets of dasatinib were observed when the U/FA.2 elution method was applied, and in all cases recovery was enhanced compared to the standard method. Well-known targets that were identified with a notably higher abundance were ABL2 and receptor tyrosine kinases (DDR1, EPHB4). Several SRC and SRC-related kinases (CSK, LYN, FYN, and c-SRC), SYK, TNK2 (ACK1) and the serine-threonine kinases, ILK, GAK, MAPK14, MAP3K3 *etc*. were also observed with higher abundance (Fig. 4D). Perhaps even more remarkable than the observations made with the covalent drug immobilization experiments, was that all the secondary interactors (excluding the robust IPP complex) were identified with lower abundance (Fig. 4D). Furthermore, for both drug coupling approaches the increase in target recovery with U/FA.2 (Fig. 6A, red circles) was particularly noticeable for tyrosine kinases (including receptor tyrosine kinases). This observation was emphasised as the target recovery of RTKs with FA elution method was particularly underwhelming. Differences in target profiles between chemically-coupled and biotinylated drug data were minor (Fig. 6A, two tones of orange). Moreover, excluding the kinases TESK (not enriched in the U/FA.2 eluate with c-dasatinib, and not identified in the c-dasatinib-biotinylated pulldowns) and ARAF (not enriched in the U/FA.2 eluate with c-dasatinib-XX-biotin, and not identified in the c-dasatinib pulldowns) (Fig. 6A, green); for all dasatinib targets U/FA.2 was more efficient than FA. Finally, the data led us to conclude that the observed improvement in the eluted protein profiles is not constrained to a particular class of kinases, but rather, to the overall increase in target capture (Fig. 6A).

4.4. Elution with the combination of formic acid and urea also improved identification of cognate targets of sunitinib

We next evaluated if the improvements observed with the U/FA.2 method were unique to dasatinib and target proteins; or if this would also translate to other drug-protein interactions. Therefore, sunitinib [34] was selected. Similar to dasatinib, this compound also has multiple targets, but the profile only displays minimal overlap with dasatinib [7,28,53]. Affinity chromatography with c-sunitinib was performed on human erythroid leukemia cells (Fig. 5A). HEL cells are known to express the RTK c-KIT, which is a cognate target of sunitinib. The data revealed that both FA and U/FA.2 elution successfully eluted c-KIT as shown by immunoblotting (Fig. 5B). Consistent with our previous observations using

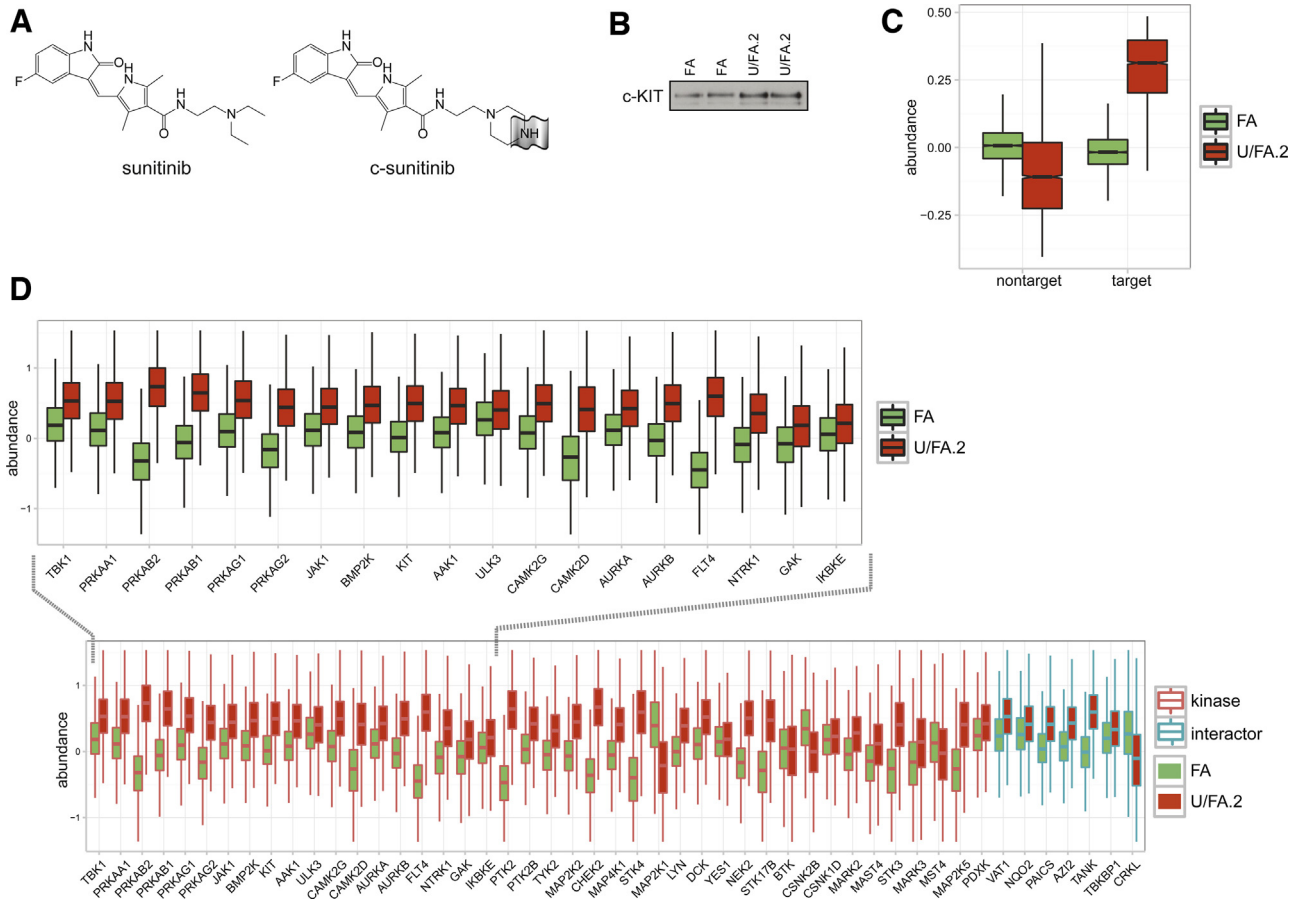

Fig. 5. Formic acid/urea double elution improved the identification of sunitinib targets. (A) Chemical structure of sunitinib and c-sunitinib. The latter is the chemically-modified version of sunitinib that can be coupled to sepharose beads via a linker. (B) Anti-KIT western blot of FA and U/FA.2 pulldowns. Immunoblot signal for U/FA.2 is stronger compared to the standard elution with 100 mM FA. (C) Comparison of overall abundances between FA and U/FA.2. A strong increase in abundance is observed for target proteins with U/FA.2. Two biological replicates were analysed (two technical replicates each). (D) The majority of cognate kinase targets of sunitinib are more abundant in U/FA.2 than FA. An integrated plot showing differences in abundances between the FA and U/FA.2 elution methods is shown. Kinases and kinase-interacting proteins are indicated in the red and blue box plots, respectively. (For interpretation of the references to color in this figure legend, the reader is referred to the web version of this article.)

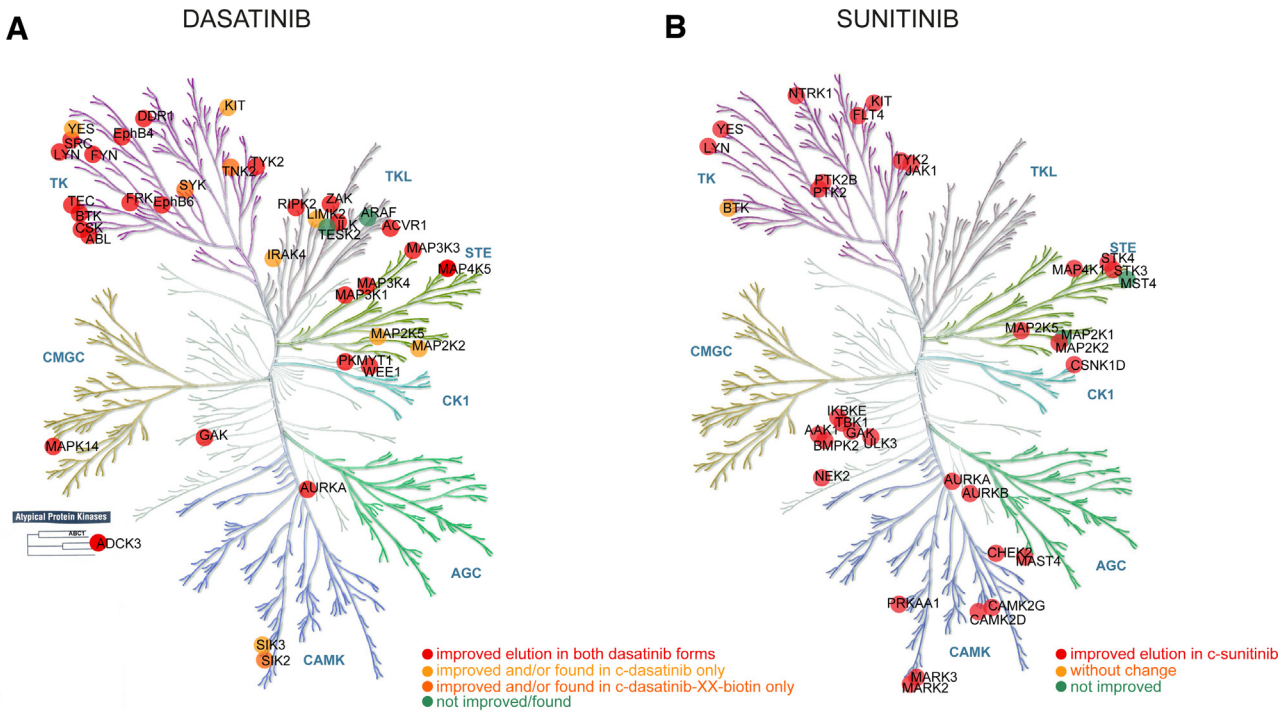

Fig. 6. Displayed on the kinome tree in red are the kinases that were observed with a higher abundance in the U/FA.2 elution method. The improvement in eluted protein profiles is not constrained to a particular class of kinases, but rather, the overall increase in target capture. (A) Kinome tree representation for both dasatinib coupling approaches. Kinases that were recovered with either c-dasatinib or c-dasatinib-XX-biotin are depicted in two different tones of orange, respectively. Kinases that had a higher recovery with the standard method are displayed in green. (B) In red are the kinases that were observed with a higher abundance in the U/FA.2 elution method in sunitinib pulldowns. The improvement in eluted protein profiles is not constrained to a particular branch and it is mostly reciprocal to dasatinib target distribution. Kinases that had same recovery are depicted in orange; the ones that had a higher recovery with the standard method are displayed in green. Illustration reproduced courtesy of Cell Signaling Technology, Inc. (www.cellsignal.com). (For interpretation of the references to color in this figure legend, the reader is referred to the web version of this article.)

dasatinib, U/FA.2 elution resulted in an improved recovery of c-KIT. Furthermore, subsequent LCMS analysis showed that both methods led to the identification of a large number of kinase targets. The overall elution efficiency across all targets, however, was dramatically enhanced with the urea/formic acid double elution (Fig. 5C). This improvement was particularly apparent when the data from other targets of sunitinib was compared, *e.g.*, c-KIT, PRKAA1 (5′-AMP-activated protein kinase 1 alpha, AMPK1α), or TBK1. As for dasatinib, this improvement was not restricted to a particular branch of the kinome tree (Fig. 6. A and B). Indirect binding proteins of kinases, such as regulatory subunits and multicomponent kinase complex partners of 5′-AMP-activated protein kinase (PRKAB1, PRKAB2, PRKAAG1, PRKAAG2 etc), orTBK1 (TANK, TBKBP1, AZI2) (Fig. 5D) also showed marked improvement. Furthermore, a number of non-dasatinib kinase targets were eluted more efficiently. These include tyrosine kinases JAK1, FLT4, NTRK1, PTK2 (FAK), PTK2B (FAK2) *etc.*; and serine/threonine NAK kinases (AAK1, BMP2K, GAK), IKK-related kinases (IKBKE, TBK1), and NEK kinases (NEK2). Calcium/calmodulin dependent protein kinases such are CAMK2D and CAMK2D were strongly enriched in the U/FA.2 eluates, in addition to CHEK2, MARK2 and MARK3. This data showed that the improvement in protein recovery observed with the U/FA double elution is widely applicable and not just restricted to a single drug or individual target protein thereof.

5. Conclusion

In this study, we report the successful optimization of chemical proteomics coupled to gel-free mass spectrometry. By introducing an adapted double elution method that is beneficial for both standard drug immobilization protocols and biotinylated drugs, we could retrieve all cognate targets with higher efficiency compared to our previously preferred method. In general, the combination of a denaturing agent with formic acid led to an increase in the elution efficiency of drug targets; despite the fact that the concentration of formic acid was 2-fold lower. The double elution with a combination of 3 M urea and 50 mM formic acid resulted in paramount target recovery without comparable enrichment of non-specific proteins. This was not constrained neither to a particular branch of the kinome dendrogram, nor to a single drug. Furthermore, the success of this elution protocol with biotinylated compounds offers a promising prospect of also capturing covalent drug-protein interactions. We believe this adapted elution method will improve the characterization of cellular target profiles of small molecules. It is mild, rapid, affordable and efficient, and allows a wide spectrum of proteins to be captured in a single chemical proteomic experiment.

Conflict of interest

The authors declare no competing financial interests.

Author contributions

The manuscript was written with contributions from all authors. All authors have given approval to the final version of manuscript.

Acknowledgment

Research in our groups at CeMM is supported by the Austrian Academy of Sciences and the ASSET project funded by the

European Union within the FP7 framework. B.R.S. is financed by the ASSET project (HEALTH-F4-2010-259348).

Appendix A. Supplementary data

Supplementary data associated with this article can be found, in the online version, at http://dx.doi.org/10.1016/j.euprot.2015.09.002.

References

[1] B.K. Wagner, P.A. Clemons, Connecting synthetic chemistry decisions to cell and genome biology using small-molecule phenotypic profiling, Curr. Opin. Chem. Biol. 13 (2009) 539–548.
[2] J. Lee, M. Bogyo, Target deconvolution techniques in modern phenotypic profiling, Curr. Opin. Chem. Biol. 17 (2013) 118–126.
[3] U. Rix, G. Superti-Furga, Target profiling of small molecules by chemical proteomics, Nat. Chem. Biol. 5 (2009) 616–624.
[4] D.A. Tuveson, N.A. Willis, T. Jacks, J.D. Griffin, S. Singer, C.D. Fletcher, et al., STI571 inactivation of the gastrointestinal stromal tumor c-KIT oncoprotein: biological and clinical implications, Oncogene 20 (2001) 5054–5058.
[5] E.J. Licitra, J.O. Liu, A three-hybrid system for detecting small ligand-protein receptor interactions, Proc. Natl. Acad. Sci. U. S. A. 93 (1996) 12817–12821.
[6] O. Hantschel, U. Rix, U. Schmidt, T. Burckstummer, M. Kneidinger, G. Schutze, et al., The Btk tyrosine kinase is a major target of the Bcr-Abl inhibitor dasatinib, Proc. Natl. Acad. Sci. U. S. A. 104 (2007) 13283–13288.
[7] M.I. Davis, J.P. Hunt, S. Herrgard, P. Ciceri, L.M. Wodicka, G. Pallares, et al., Comprehensive analysis of kinase inhibitor selectivity, Nat. Biotechnol. 29 (2011) 1046–1051.
[8] K. Godl, J. Wissing, A. Kurtenbach, P. Habenberger, S. Blencke, H. Gutbrod, et al., An efficient proteomics method to identify the cellular targets of protein kinase inhibitors, Proc. Natl. Acad. Sci. U. S. A. 100 (2003) 15434–15439.
[9] J. Drews, Case histories, magic bullets and the state of drug discovery, Nat. Rev. Drug Discov. 5 (2006) 635–640.
[10] C. Chidley, H. Haruki, M.G. Pedersen, E. Muller, K. Johnsson, A yeast-based screen reveals that sulfasalazine inhibits tetrahydrobiopterin biosynthesis, Nat. Chem. Biol. 7 (2011) 375–383.
[11] J. Lamb, E.D. Crawford, D. Peck, J.W. Modell, I.C. Blat, M.J. Wrobel, et al., The connectivity map: using gene-expression signatures to connect small molecules, genes, and disease, Science 313 (2006) 1929–1935.
[12] G.C. Adam, E.J. Sorensen, B.F. Cravatt, Trifunctional chemical probes for the consolidated detection and identification of enzyme activities from complex proteomes, Mol. Cell. Proteomics 1 (2002) 828–835.
[13] H. Daub, K. Godl, D. Brehmer, B. Klebl, G. Muller, Evaluation of kinase inhibitor selectivity by chemical proteomics, Assay Drug Dev. Technol. 2 (2004) 215–224.
[14] D.A. Jeffery, M. Bogyo, Chemical proteomics and its application to drug discovery, Curr. Opin. Biotechnol. 14 (2003) 87–95.
[15] H. Katayama, Y. Oda, Chemical proteomics for drug discovery based on compound-immobilized affinity chromatography, J. Chromatogr. B 855 (2007) 21–27.
[16] U. Kruse, M. Bantscheff, G. Drewes, C. Hopf, Chemical and pathway proteomics: powerful tools for oncology drug discovery and personalized health care, Mol. Cell. Proteomics 7 (2008) 1887–1901.
[17] S.-E. Ong, M. Schenone, A.A. Margolin, X. Li, K. Do, M.K. Doud, et al., Identifying the proteins to which small-molecule probes and drugs bind in cells, Proc. Natl. Acad. Sci. U. S. A. 106 (2009) 4617–4622.
[18] J. Rappsilber, M. Mann, Analysis of the topology of protein complexes using cross-linking and mass spectrometry, CSH Protoc. 2007 (2007) pdb prot4594.
[19] Y. Oda, T. Owa, T. Sato, B. Boucher, S. Daniels, H. Yamanaka, et al., Quantitative chemical proteomics for identifying candidate drug targets, Anal. Chem. 75 (2003) 2159–2165.
[20] D. Brehmer, Z. Greff, K. Godl, S. Blencke, A. Kurtenbach, M. Weber, et al., Cellular targets of gefitinib, Cancer Res. 65 (2005) 379–382.
[21] U. Rix, O. Hantschel, G. Durnberger, L.L. Remsing Rix, M. Planyavsky, N.V. Fernbach, et al., Chemical proteomic profiles of the BCR-ABL inhibitors imatinib, nilotinib, and dasatinib reveal novel kinase and nonkinase targets, Blood 110 (2007) 4055–4063.
[22] P.L. Ross, Y.N. Huang, J.N. Marchese, B. Williamson, K. Parker, S. Hattan, et al., Multiplexed protein quantitation in *Saccharomyces cerevisiae* using amine-reactive isobaric tagging reagents, Mol. Cell. Proteomics 3 (2004) 1154–1169.
[23] N.V. Fernbach, M. Planyavsky, A. Muller, F.P. Breitwieser, J. Colinge, U. Rix, et al., Acid elution and one-dimensional shotgun analysis on an orbitrap mass spectrometer: an application to drug affinity chromatography, J. Proteome Res. 8 (2009) 4753–4765.
[24] E.B. Haura, A. Muller, F.P. Breitwieser, J. Li, F. Grebien, J. Colinge, et al., Using iTRAQ combined with tandem affinity purification to enhance low-abundance proteins associated with somatically mutated EGFR core complexes in lung cancer, J. Proteome Res. 10 (2011) 182–190.
[25] G.E. Winter, U. Rix, S.M. Carlson, K.V. Gleixner, F. Grebien, M. Gridling, et al., Systems-pharmacology dissection of a drug synergy in imatinib-resistant CML, Nat. Chem. Biol. 8 (2012) 905–912.
[26] G.E. Winter, U. Rix, A. Lissat, A. Stukalov, M.K. Mullner, K.L. Bennett, et al., An integrated chemical biology approach identifies specific vulnerability of Ewing's sarcoma to combined inhibition of aurora kinases A and B, Mol. Cancer Ther. 10 (2011) 1846–1856.
[27] K.V. Huber, E. Salah, B. Radic, M. Gridling, J.M. Elkins, A. Stukalov, et al., Stereospecific targeting of MTH1 by (S)-crizotinib as an anticancer strategy, Nature 508 (2014) 222–227.
[28] M. Gridling, S. Ficarro, F.P. Breitwieser, L. Song, K. Parapatics, J. Colinge, et al., Identification of kinase inhibitor targets in the lung cancer microenvironment by chemical and phosphoproteomics, Mol. Cancer Ther. (2014) .
[29] U. Rix, J. Colinge, K. Blatt, M. Gridling, Rix L.L. Remsing, K. Parapatics, et al., A target-disease network model of second-generation BCR-ABL inhibitor action in Ph+ ALL, PLoS One 8 (2013) e77155.
[30] V. Borgdorff, U. Rix, G.E. Winter, M. Gridling, A.C. Muller, F.P. Breitwieser, et al., A chemical biology approach identifies AMPK as a modulator of melanoma oncogene MITF, Oncogene 33 (2014) 2531–2539.
[31] L.J. Lombardo, F.Y. Lee, P. Chen, D. Norris, J.C. Barrish, K. Behnia, et al., Discovery of *N*-(2-chloro-6-methyl-phenyl)-2-(6-(4-(2-hydroxyethyl)-piperazin-1-yl)-2-methylpyrimidin-4-ylamino) thiazole-5-carboxamide (BMS-354825), a dual Src/Abl kinase inhibitor with potent antitumor activity in preclinical assays, J. Med. Chem. 47 (2004) 6658–6661.
[32] M. Kneidinger, U. Schmidt, U. Rix, K.V. Gleixner, A. Vales, C. Baumgartner, et al., The effects of dasatinib on IgE receptor–dependent activation and histamine release in human basophils, Blood 111 (2008) 3097–3107.
[33] J. Li, U. Rix, B. Fang, Y. Bai, A. Edwards, J. Colinge, et al., A chemical and phosphoproteomic characterization of dasatinib action in lung cancer, Nat. Chem. Biol. 6 (2010) 291–299.
[34] L. Sun, C. Liang, S. Shirazian, Y. Zhou, T. Miller, J. Cui, et al., Discovery of 5-[5-fluoro-2-oxo-1,2- dihydroindol-(3Z)-ylidenemethyl]-2,4-dimethyl-1H-pyrrole-3-carboxylic acid (2-diethylaminoethyl) amide, a novel tyrosine kinase inhibitor targeting vascular endothelial and platelet-derived growth factor receptor tyrosine kinase, J. Med. Chem. 46 (2003) 1116–1119.
[35] J. Hartmann, L. Kanz, Sunitinib and periodic hair depigmentation due to temporary c-kit inhibition, Arch. Dermatol. 144 (2008) 1525–1526.
[36] R. Kumar, M.C. Crouthamel, D.H. Rominger, R.R. Gontarek, P.J. Tummino, R.A. Levin, et al., Myelosuppression and kinase selectivity of multikinase angiogenesis inhibitors, Br. J. Cancer 101 (2009) 1717–1723.
[37] T. Burckstummer, K.L. Bennett, A. Preradovic, G. Schutze, O. Hantschel, G. Superti-Furga, et al., An efficient tandem affinity purification procedure for interaction proteomics in mammalian cells, Nat. Methods 3 (2006) 1013–1019.
[38] J. Rappsilber, Y. Ishihama, M. Mann, Stop and go extraction tips for matrix-assisted laser desorption/ionization, nanoelectrospray, and LC/MS sample pretreatment in proteomics, Anal. Chem. 75 (2003) 663–670.
[39] K.L. Bennett, M. Funk, M. Tschernutter, F.P. Breitwieser, M. Planyavsky, C. Ubaida Mohien, et al., Proteomic analysis of human cataract aqueous humour: comparison of one-dimensional gel LCMS with two-dimensional LCMS of unlabelled and iTRAQ(R)-labelled specimens, J. Proteomics 74 (2011) 151–166.
[40] J.V. Olsen, L.M. de Godoy, G. Li, B. Macek, P. Mortensen, R. Pesch, et al., Parts per million mass accuracy on an Orbitrap mass spectrometer via lock mass injection into a C-trap, Mol. Cell. Proteomics 4 (2005) 2010–2021.
[41] Y. Zhang, Z. Wen, M.P. Washburn, L. Florens, Refinements to label free proteome quantitation: how to deal with peptides shared by multiple proteins, Anal. Chem. 82 (2010) 2272–2281.
[42] Stan Development Team. Stan: A C^{++} Library for Probability and Sampling, Version 2.4 2014.
[43] L.O. Narhi, D.J. Caughey, T. Horan, Y. Kita, D. Chang, T. Arakawa, Effect of three elution buffers on the recovery and structure of monoclonal antibodies, Anal. Biochem. 253 (1997) 236–245.
[44] B.S. Parekh, H.B. Mehta, M.D. West, R.C. Montelaro, Preparative elution of proteins from nitrocellulose membranes after separation by sodium dodecyl sulfate-polyacrylamide gel electrophoresis, Anal. Biochem. 148 (1985) 87–92.
[45] M.J. Towle, K.A. Salvato, J. Budrow, B.F. Wels, G. Kuznetsov, K.K. Aalfs, et al., In vitro and in vivo anticancer activities of synthetic macrocyclic ketone analogues of halichondrin B, Cancer Res. 61 (2001) 1013–1021.
[46] J. Colinge, U. Rix, K.L. Bennett, G. Superti-Furga, Systems biology analysis of protein-drug interactions, Proteomics Clin. Appl. 6 (2012) 102–116.
[47] O. Hantschel, U. Rix, G. Superti-Furga, Target spectrum of the BCR-ABL inhibitors imatinib, nilotinib and dasatinib, Leuk. Lymphoma 49 (2008) 615–619.
[48] M. Bantscheff, D. Eberhard, Y. Abraham, S. Bastuck, M. Boesche, S. Hobson, et al., Quantitative chemical proteomics reveals mechanisms of action of clinical ABL kinase inhibitors, Nat. Biotechnol. 25 (2007) 1035–1044.
[49] L.C. Kim, U. Rix, E.B. Haura, Dasatinib in solid tumors, Expert Opin. Investig. Drugs 19 (2010) 415–425.
[50] L.L. Remsing Rix, U. Rix, J. Colinge, O. Hantschel, K.L. Bennett, T. Stranzl, et al., Global target profile of the kinase inhibitor bosutinib in primary chronic myeloid leukemia cells, Leukemia 23 (2009) 477–485.
[51] E.K. Greuber, P. Smith-Pearson, J. Wang, A.M. Pendergast, Role of ABL family kinases in cancer: from leukaemia to solid tumours, Nat. Rev. Cancer 13 (2013) 559–571.
[52] K.R. Legate, E. Montanez, O. Kudlacek, R. Fassler, ILK, PINCH and parvin: the tIPP of integrin signalling, Nat. Rev. Mol. Cell Biol. 7 (2006) 20–31.
[53] T. Anastassiadis, S.W. Deacon, K. Devarajan, H. Ma, J.R. Peterson, Comprehensive assay of kinase catalytic activity reveals features of kinase inhibitor selectivity, Nat. Biotechnol. 29 (2011) 1039–1045.